LABORATORI NAZIONALI DI FRASCATI
SIS – Pubblicazioni

LNF-00/036 (P)
18 Dicembre 2000

VELOCITY BUNCHING IN PHOTO-INJECTORS

L. Serafini[1], M. Ferrario[2]

[1)]INFN- Sezione di Milano, Via Celoria 16, 20133 Milano, Italy
[2)]INFN- Laboratori Nazionali di Frascati, Via E. Fermi 40, 00044 Frascati (Roma), Italy

Abstract

We describe here a new method to increase the peak current of high brightness electron beams as those required to drive X-ray SASE FEL's, that is based on a rectilinear compressor scheme utilizing the bunching properties of slow waves. It is shown that whenever a beam, slower than the synchronous velocity, is injected into a RF wave at the zero acceleration phase and slips back in phase up to the peak acceleration phase, it can be compressed as far as the extraction happens at the synchronous velocity. In fact, the bunch undergoes a quarter of synchrotron oscillation that induces a net compression (i.e. a bunch length reduction) up to a factor of 20 when proper care is taken to preserve the longitudinal emittance. A few examples are presented to demonstrate the potentialities of this method, by which multi-kA beams at very low emittance can be generated at moderate energies (about 100 MeV).

PACS.: 29.27.Bd

Presented at the: 20th ICFA Beam Dynamics Workshop on
"Physics of, and Science with, the X-ray Free-Electron Laser"
Arcidosso (Italy), Settembre 10-15, 2000

1 INTRODUCTION

The need to produce high brightness electron beams delivered in short (sub picosecond) bunches has been driven recently by the demands of X-ray SASE FEL's, which typically require multi-GeV beams with multi-kA peak currents and bunch lengths in the 100-300 fs range, associated to normalized transverse emittances lower than a few mm·mrad.

The foreseen strategy to attain those beams is based in present designs on the use of RF Linacs in conjunction with RF laser driven Photoinjectors and magnetic compressors. The formers are needed as sources of low emittance high charge beams (usually 2 mm·mrad at 1 nC bunch charge) with moderate currents (< 100 A @ 10 MeV), the latter are used to enhance the peak current of such beams up to the design value of 2-3 kA by reduction of the bunch length achieved at relativistic energies (> 300 MeV, up to 5 GeV in multi-staged compressors).

Since the impact of magnetic compressors on the beam dynamics is quite relevant, with tendency to jeopardize the performances of the whole system in terms of the final beam brightness achieved – this makes these type of compressors one of the critical components of these Linacs – we tried to explore an alternative option of compression (i.e. of current enhancement) based on slow wave RF fields.

The performances of this option are presented in this paper on the basis of a preliminary analysis, whose main conclusion is that this method of compression has very promising potentialities and is a good candidate to substitute magnetic compressors, alleviating in this way the problems related to Coherent Synchrotron Radiation emission occurring in the chicanes of magnetic compressors and its critical impact on the beam quality (brightness) achievable.

The great advantage of the RF rectilinear compressor scheme presented here is obviously the absence of curved path trajectories in the compressor, in addition to the fact that compression is applied at moderate energies (from 10 to 100 MeV), leaving the Linac (up to the final energy) free from any further beam manipulation needed to increase the current.

The rectilinear RF compressor works indeed as a standard accelerating structure which, while accelerates the beam, it also reduces its bunch length.

We have to acknowledge here that the seed of the idea leading to the RF compressor was set in the development of a previous work on a plasma buncher scheme[1] which turned out to be of great relevance for the studies on second generation plasma accelerators[2].

In that work indeed it was shown that a plasma accelerator working at some resonant gamma γ_r can accelerate and simultaneously compress long bunches injected at a proper phase, i.e. the phase of no net acceleration. In that specific example, a plasma wave driven at an amplitude of 3 GV/m with plasma wavelength of 300 μm accelerates an electron bunch injected at 2.5 MeV up to an energy of 200 MeV, by simultaneously reducing the bunch length from 15 μm at injection down to 3 μm . In order to achieve this effect is necessary to inject at 0° phase (no acceleration) so to let the beam slip back in phase and extract the beam when its energy is close to the resonant gamma of the wave (in this case $\gamma_r = 400$). In case of injection at 90° (max acceleration) the bunch would be accelerated up to a higher final energy (290 MeV) but its length would be left unchanged.

The longitudinal component E_z of the RF field in a traveling wave structure or a Langmuir wave in a cold plasma can be well approximated by a simple expression neglecting higher order

spatial harmonics

$$E_z = -E_0 \sin(\omega t - kz + \psi_0) \tag{1}$$

where the wave number k is taken to be $k = \frac{\omega}{\beta_r c}$ (implying a wave phase velocity given by $v_r = \beta_r c$, $\gamma_r = 1/\sqrt{1-\beta_r^2}$) and the wave amplitude E_0 can be cast in terms of a dimensionless parameter α , defined as $\alpha \equiv \frac{eE_0}{mc^2 k}$, which represents the normalized amplitude of the vector potential associated to the wave electric field (we are considering here waves with phase velocity quite close to c, or, in other words, resonant gamma's quite large, $\gamma_r >> 1$).

The interaction between an electron and a wave of this kind can be described by an Hamiltonian

$$H = \gamma - \beta_r \sqrt{\gamma^2 - 1} - \alpha \cos\xi \tag{2}$$

where γ is the normalized energy of the electron, $\gamma = 1 + \frac{T}{mc^2}$ and $\xi = kz - \omega t - \psi_0$ the phase of the wave as seen by the electron.

Let us consider now a wave whose phase velocity is slightly smaller than c, so that $k = k_0 + \Delta k = \frac{\omega}{c} + \Delta k$, and the detuning parameter Δk is small, i.e. $\Delta k << k_0$; the resonant beta and gamma can be well approximated by

$$\beta_r \cong 1 - \frac{\Delta k}{k_0} = 1 - \frac{c\Delta k}{\omega} \qquad \text{and} \qquad \gamma_r \cong \sqrt{\frac{k_0}{2\Delta k}} = \sqrt{\frac{\omega}{2c\Delta k}} \tag{3}$$

In previous example related to the plasma wave accelerator we have $\gamma_r = 400$, so the detuning parameter is $\Delta k = 3.1 \cdot 10^{-6} k_0$.

The trapping and acceleration in these waves has been widely discussed in the literature (see for example in ref.3), and it can be well understood looking at the phase contour plots in the $[\gamma, \xi]$ phase space. One of the most relevant feature is that whenever the resonant gamma is finite, i.e. the wave is slower than c, we have a separatrix in this space, splitting trapped orbits from untrapped ones.

This situation is illustrated in Fig.1 for the case of a wave of amplitude $\alpha = 0.2$ and resonant gamma $\gamma_r = 12$. This corresponds to a wave phase velocity of $\beta_r = 0.9965$ or an equivalent detuning parameter of $\Delta k = 3.5 \cdot 10^{-3} k_0$. The top of the separatrix (i.e. the value of γ at $\xi = 0$ for $\gamma_0 = \gamma_r$ and $\psi_0 = \pi$) is approximately given by $\gamma_{\max} = 4\alpha\gamma_r^2$, which is the maximum energy of trapped particles .

Since the Hamiltonian written in eq.2 is an invariant of the motion, we can evaluate it at injection, getting:

$$\gamma - \beta_r \sqrt{\gamma^2 - 1} - \alpha \cos\xi = \gamma_0 - \beta_r \sqrt{\gamma_0^2 - 1} - \alpha \cos\psi_0 \tag{4}$$

where γ_0 and ψ_0 are the initial energy and phase of the particle injected into the wave.

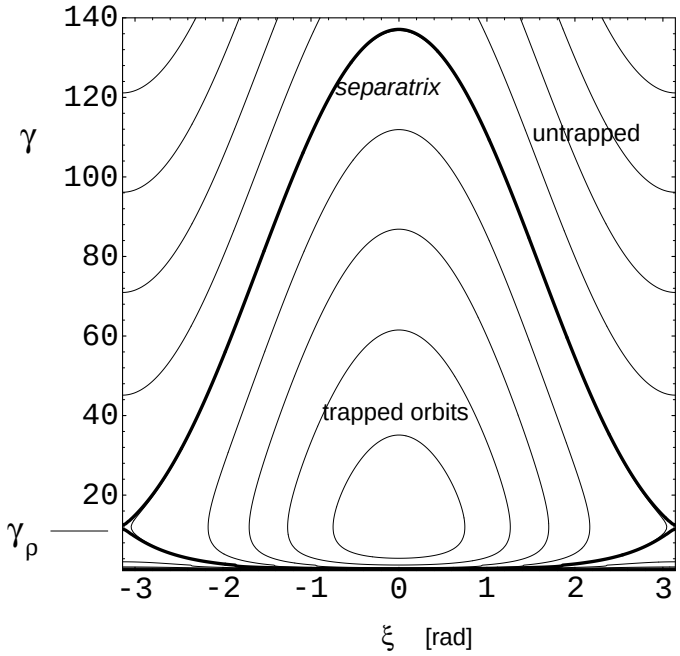

FIG. 1: Phase space plots for a slow wave with resonant gamma $\gamma_r = 12$ and $\alpha = 0.2$. The separatrix is shown by the bolded line.

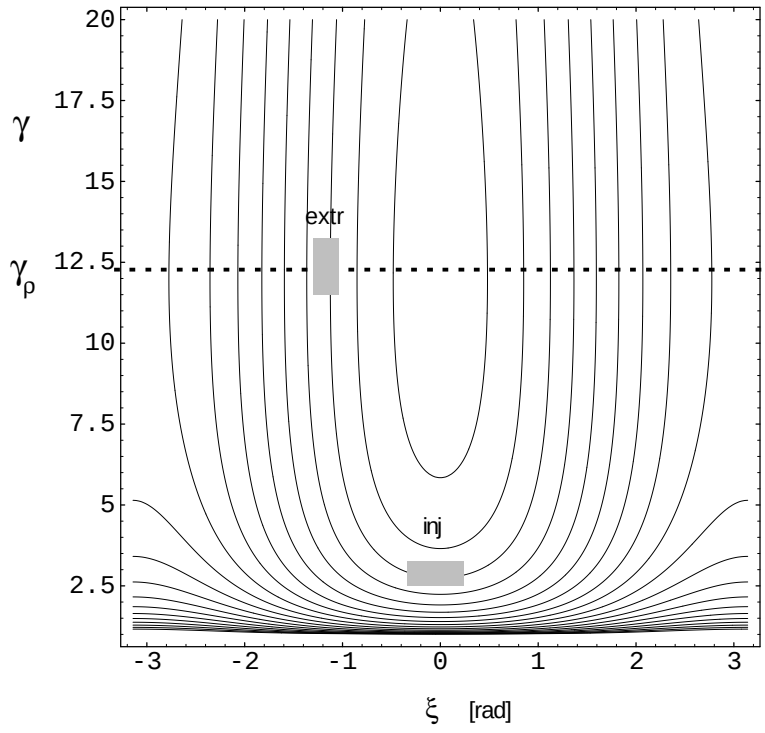

FIG. 2: Enlarged part of the diagram plotted in Fig.1, corresponding to $\gamma \leq 20$.

The maximum accelerating gradient occurs at $\xi = -\pi/2$: if particles are injected at this phase inside the separatrix region with an initial energy γ_0 smaller than the resonant one γ_r they will slip back in phase but they will be accelerated up to $\gamma = \gamma_r$, where their velocity will match that of the wave, thereafter they will start to slip ahead of the wave during the acceleration up to the highest γ value of their phase contour line (well above γ_r) corresponding to $\xi = 0$. At this point they will start being decelerated unless extracted from the wave.

There is one relevant property of this kind of energy oscillation performed into the bucket by trapped electrons, which turns out to be very helpful in reducing the phase distance of particles injected close to each other into the wave at small energy.

Because of the shape of the phase contour lines, the region around $\xi = 0$ corresponds to high phase spreads and low energy spreads while the opposite is true for the region around $\xi = -\pi/2$ where the phase lines are parallel to the γ-axis.

This is quite well illustrated in Fig.2 where an enlarged part of the diagram plotted in Fig.1 is shown, and exactly that corresponding to $\gamma \le 20$. In this figure a particle distribution at injection is depicted in a small phase space area located around $\xi = 0$ and $\gamma_0 = 3$, i.e. well below γ_r (i.e. particles initially slower than the wave) and close to the bottom of the cup-shaped bucket. This bunch of particles is accelerated by the wave while it slips back in phase: once at the resonant energy γ_r it will reach a phase of about $\xi = -60^o$. As depicted in the diagram, due to the nature of the phase lines, the bunch will have a phase spread (i.e. a bunch length since it is quite relativistic at this point) smaller than the initial one, which means that this kind of acceleration acts also as a phase compression.

Extracting the bunch when it reaches γ_r is therefore the way to achieve a bunch length compression at the same time as acceleration: a further acceleration beyond γ_r would clearly tend to de-compress the bunch, as clearly shown by the shape of the phase lines above γ_r (inside the separatrix).

We can evaluate the amount of phase compression achieved by assuming injection at $\xi = 0$ and extraction at $\gamma = \gamma_r$, so that eq.4 becomes

$$\frac{1}{\gamma_r} - \alpha\cos\xi_{ex} = \gamma_0 - \beta_r\sqrt{\gamma_0^2 - 1} - \alpha \tag{5}$$

which basically determines the extraction phase ξ_{ex} as a function of the injection conditions (γ_0, ψ_0) and the wave parameters (γ_r, α) .

We also assume that the injection phase ψ_0 and energy γ_0 will be distributed around some average values $\bar{\gamma}_0$ and $\bar{\psi}_0$ with rms spreads defined as $\gamma_0 = \bar{\gamma}_0 \pm \delta\gamma_0$ and $\psi_0 = \bar{\psi}_0 \pm \delta\psi_0$. These initial spreads in energy and phase at injection will affect the final phase spread $\delta\xi_{ex}$ at extraction as given by $\alpha\cos\left(\bar{\xi}_{ex} \pm \delta\xi_{ex}\right) = 1/\gamma_r - \left(\bar{\gamma}_0 \pm \delta\gamma_0\right) + \beta_r\sqrt{\left(\bar{\gamma}_0 \pm \delta\gamma_0\right)^2 - 1} + \alpha\cos\left(\pm\delta\psi_0\right)$, which can be cast, through a second order expansion, in the form

$$\delta\xi_{ex} = \frac{1}{2\left|\sin\bar{\xi}_{ex}\right|}\sqrt{\delta\psi_0^4 + \left(\frac{1}{\alpha\bar{\gamma}_0}\frac{\delta\gamma_0}{\bar{\gamma}_0}\right)^2\left(\frac{\bar{\gamma}_0^2}{\gamma_r^2} - 1\right)^2} \tag{6}$$

where the extraction phase is specified by $\cos\bar{\xi}_{ex} = 1 + \frac{1}{\alpha\gamma_r} - \frac{\bar{\gamma}_0}{\alpha}\left(1 - \beta_r\bar{\beta}_0\right)$.

The relevant parameter is the compression factor C, sort of a figure of merit for this process, defined as the ratio between the initial phase spread and the final one at extraction, i.e.

$C \equiv \frac{\delta\psi_0}{\delta\xi_{ex}}$, which turns out to be given by

$$C = \frac{2\delta\psi_0 \left|\sin\bar{\xi}_{ex}\right|}{\sqrt{\delta\psi_0^4 + \left(\frac{1}{\alpha\bar{\gamma}_0}\frac{\delta\gamma_0}{\bar{\gamma}_0}\right)^2}} \tag{7}$$

where we assumed $\frac{\bar{\gamma}_0^2}{\gamma_r^2} << 1$.

Taking the example shown in Fig.2, i.e. a bunch injected at $\bar{\gamma}_0 = 3$ with $\frac{\delta\gamma_0}{\bar{\gamma}_0} = 5\cdot 10^{-3}$ and $\delta\psi_0 = 5\cdot 10^{-2}$ into a wave specified by $\alpha = 0.2$ and $\gamma_r = 12$, we derive from eq.7 a compression factor $C = 9.8$, at an extraction phase $\bar{\xi}_{ex} = -60^o$, which indicates a quite interesting capability to increase the peak current in the bunch by a relevant factor (in excess of 10).

Taking as a second example the one considered in the work on plasma bunchers, i.e. a bunch injected at $\bar{\gamma}_0 = 6$ with $\frac{\delta\gamma_0}{\bar{\gamma}_0} = 5\cdot 10^{-3}$ and $\delta\psi_0 = 0.31$ (a bunch 15 μm long into a plasma wave with 300 μm wavelength) into a wave specified by $\alpha = 0.28$ (3GV/m amplitude) and $\gamma_r = 400$, we derive from eq.7 a compression factor $C = 4.5$, at an extraction phase $\bar{\xi}_{ex} = -45^o$, which is very close to the factor 5 in bunch length reduction observed in the numerical simulations, that foresee a final bunch length of 3 μm at the exit of the plasma wave[1] .

2 RF RECTILINEAR COMPRESSORS

On the basis of the bunch compression mechanism described above we can envisage a very useful application of this concept in the frame of high brightness photoinjectors for X-ray FEL drivers.

The aim of the idea is to try compressing the beam right after the exit from the RF gun, when the energy is about 5-7 MeV, by injecting the bunch into an accelerating structure which supports a slow wave like the one specified in eq.1, so that the beam would leave this structure at the final maximum value of peak current achievable at an energy close to (or somewhat higher) than the resonant gamma. If this exit energy is high enough we can envisage that the residual longitudinal space charge field will not debunch the beam further on, in particular if the beam is promptly injected into a regular high gradient accelerating structure in order to relativistically freeze down the residual - generally weak – longitudinal space charge forces.

We will consider here the lay-out of the injector for the LCLS[4], which is one of the most promising designs for high brightness beams recently proposed[5], based on the use of S-band traveling wave structures boosting a 6.5 MeV beam produced by the RF gun. The paradigm for this beam is: 1 nC bunch charge, 10 ps laser pulse length on the photocathode, 140 MV/m peak field on the photocathode, resulting in a 100 A peak current at the gun exit with 0.8 % energy spread and 0.5 mm·mrad rms normalized transverse emittance (as predicted by simulations). A solenoid lens located right at the gun exit focuses down the beam in order to match its envelope onto the invariant envelope[7] at the injection in the first TW structure, which is located 1.5 m far from the cathode[5]. We just take this lay-out and substitute the first TW structure with one that

is properly designed to support a slow wave with wave number 0.07 % higher than the nominal one (corresponding to a cell length 0.07 % shorter than the standard $\lambda/3$ nominal value of a $2\pi/3$ mode – this perturbative change in wave number is equivalent to a 2 MHz detuning of the structure, i.e. to having a 2854 MHz field propagating through a standard S-band SLAC structure). This structure will have 86 cells over a length of about 3 m, operating at 2856 MHz.

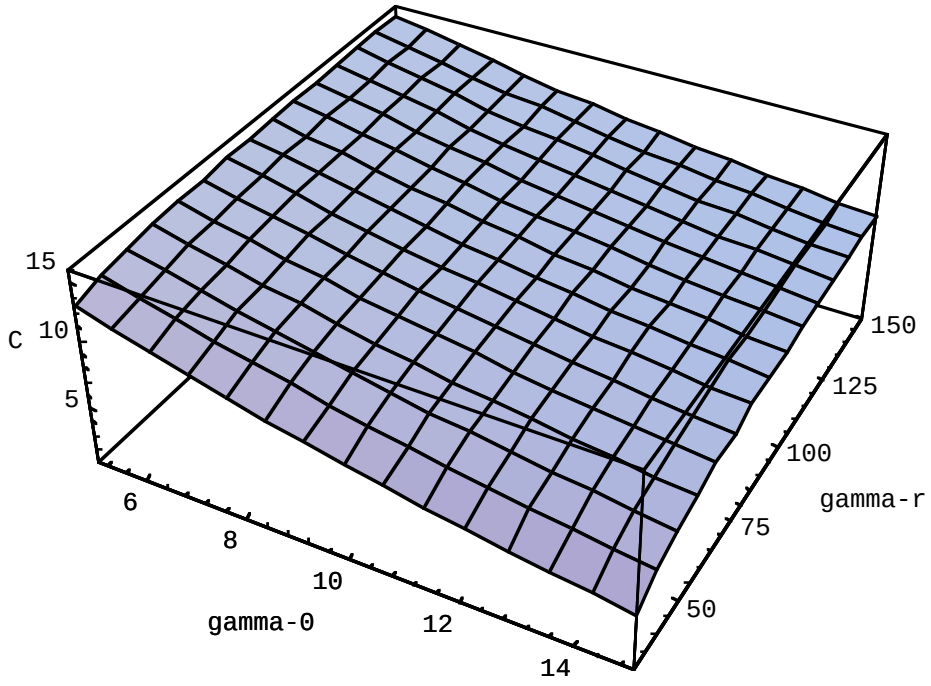

FIG. 3: Compression factor C as a function of the initial energy γ_0 and the resonant gamma γ_r for a wave of amplitude $\alpha = 0.75$ and an injected bunch characterized by $\delta\gamma_0/\bar{\gamma}_0 = 8\cdot10^{-3}$ and $\delta\psi_0 = 5\cdot10^{-2}$ (LCLS parameters at the gun exit).

As shown in Fig.3, the compression factor C for a wave of amplitude $\alpha = 0.75$ (corresponding to an accelerating gradient of 23 MV/m at S-band) is a decreasing function of γ_0 for a given γ_r and increases slightly with γ_r for a given γ_0 .

Since in the LCLS injector case the initial energy is $\gamma_0 = 14$ and the available TW structures are 3 m long, we picked up the following optimum parameters for the slow wave structure: $\gamma_r = 27$, corresponding actually to the previously mentioned 0.07 % increase in wave number and $\alpha = 0.75$. For this set of parameters the predicted compression factor is $C = 6.5$.

By optimizing the injection phase, we ran Homdyn [6] from the cathode surface all the way through the gun, drift, slow wave structure, up to the exit of a second 3 m long TW structure (regular one, no detuning, driven at 27 MV/m accelerating gradient), located right after the first detuned one. At the optimum phase (slightly earlier than 0°) we found a very nice final peak current of 870 A at an energy of 120 MeV, as shown in Fig.4.

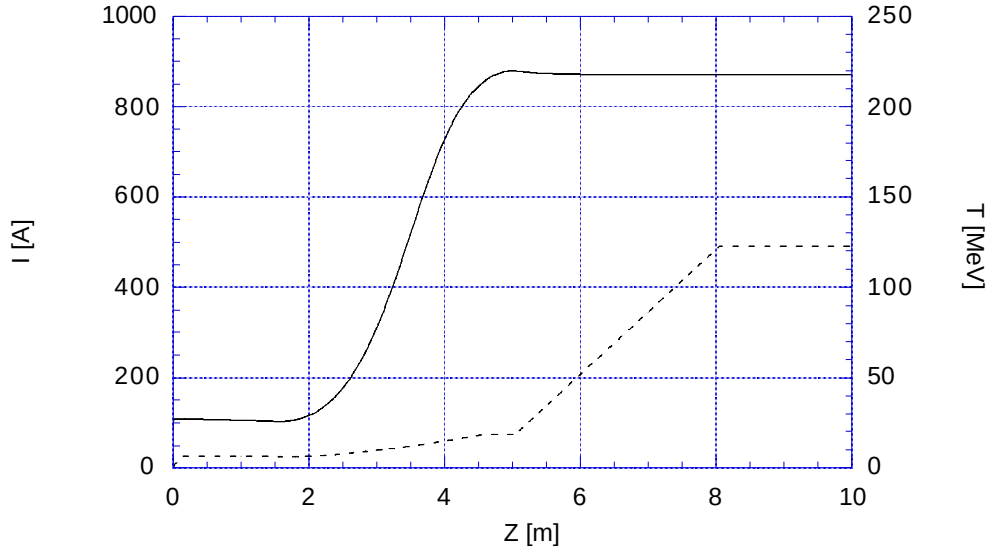

FIG. 4: Beam current (solid line, left scale, in A) and energy evolution (dashed line, right scale, in MeV) through the LCLS injector with implementation of a RF rectilinear compressor.

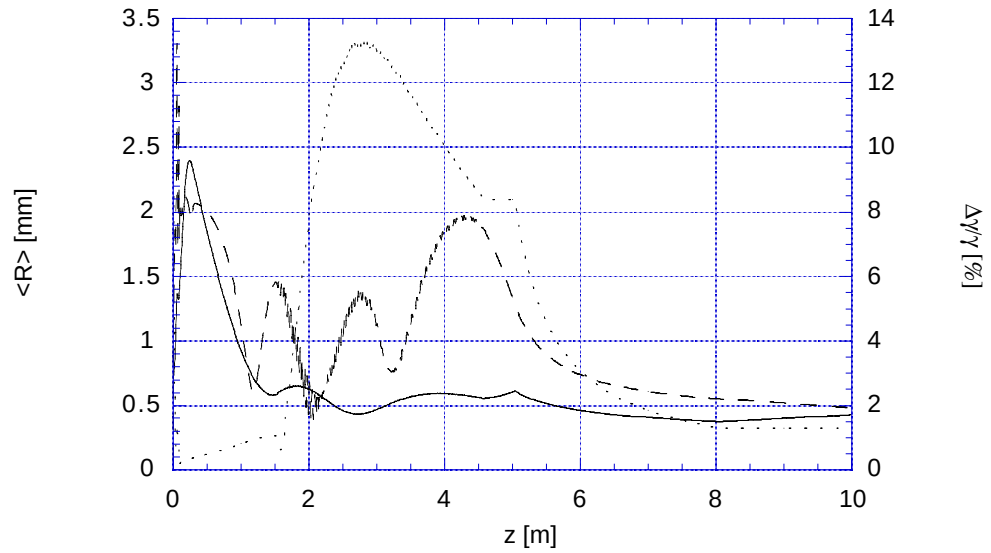

FIG. 5. Energy spread in % (dotted line, right scale), beam envelope in mm (solid line, left scale) and rms normalized transverse emittance in mm·mrad (dashed line, left scale) evolution as for Fig.4.

The effect of the RF rectilinear compressor (the detuned structure), extending from z=1.5 m up to z=4.5 m, is clearly illustrated: the energy at its exit is 18.5 MeV ($\gamma = 37$, somewhat larger than γ_r) and the compression takes place almost entirely during the acceleration through it. The compression factor achieved is $C = 8.1$, a bit larger than the analytical prediction[10].

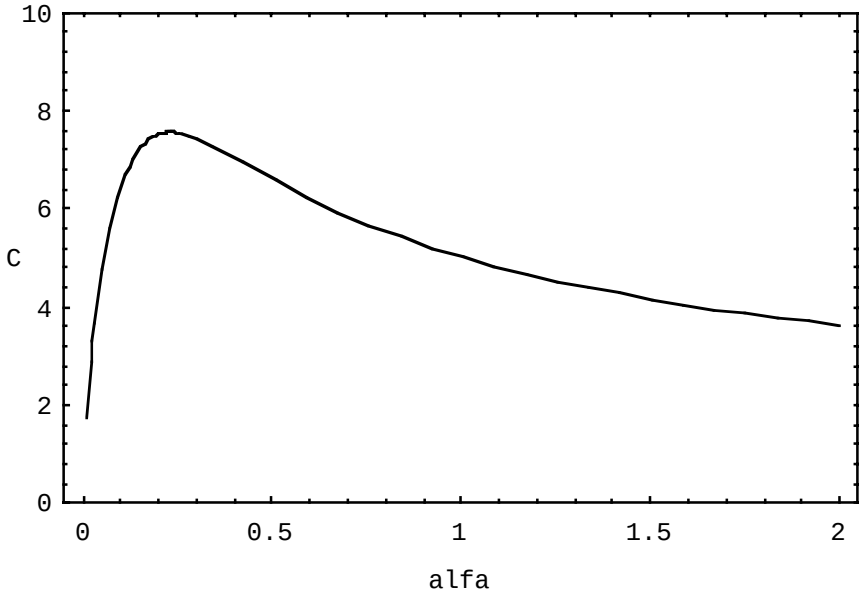

FIG. 6: Compression factor C plotted as a function of α for the same beam conditions at injection and slow wave structure used in Fig.4-5.

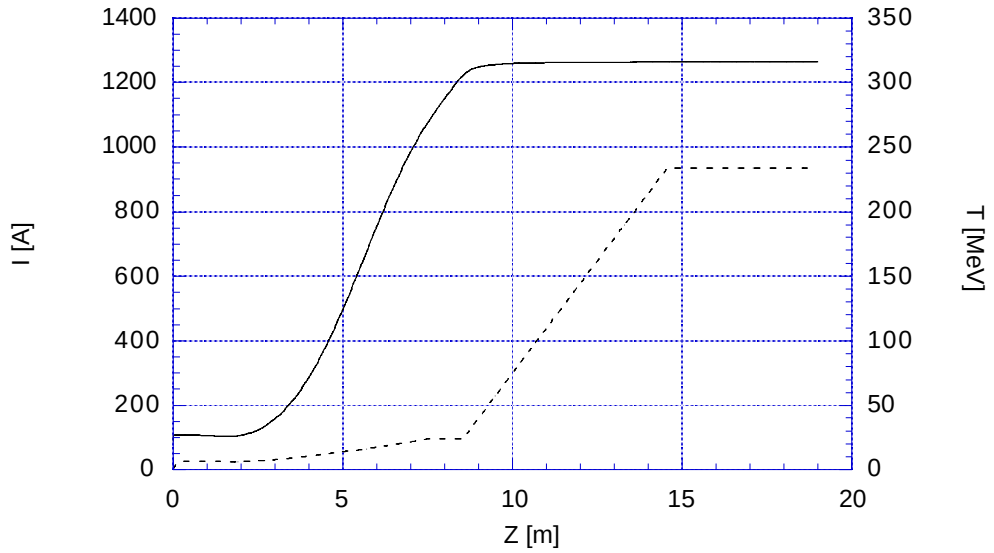

FIG. 7: Beam current (solid line) and energy evolution (dashed line, right scale) through the LCLS injector with implementation of a 6 m long RF compressor driven at low accelerating gradient.

The energy spread is plotted in Fig.5: after a large peak due to the injection at 0° phase, where the dominant effect is to induce energy spread instead of accelerating the bunch, it is naturally damped by acceleration, reaching about 1% at the exit.

The transverse dynamics is strongly altered by the compressor because the beam is all the way space charge dominated in the transverse plane: the plasma oscillation shown by the beam envelope in Fig.5 must be carefully taken under control by the solenoids wrapped around the two

accelerating sections (by proper tuning of their field amplitude) so to achieve an emittance correction scheme[7] that extends through the two accelerating structures up to 120 MeV. The final value reached, 0.5 mm·mrad, is consistent with the design value reported for the LCLS injector study, showing that the optimal emittance correction can be achieved even in presence of the RF compressor.

The rms longitudinal emittance (not shown in the figures) goes from 25 keV·mm at the exit of the RF gun up to 155 keV·mm at the exit of the RF compressor: we believe that this is due to the non-linear behavior of the accelerating field versus the accelerating phase that introduces a curvature in the longitudinal phase space. The contribution of the longitudinal space charge forces is indeed negligible throughout the RF compressor: in fact, repeating the simulation shown in Fig. 4-5 by switching off the space charge at the injection into the compressor we have obtained results almost identical to the previous case (actually the final value of the peak current is slightly smaller – 860 A – for the zero space charge case, as for the longitudinal emittance).

Therefore, if the maximum peak current achievable is limited by RF non-linearities there should be two ways to overcome this problem: one is the decrease in the accelerating gradient the second is the use of higher harmonics to flatten-out the energy-phase correlation [8].

We will discuss the second option in the next section of this paper: let us now consider what is the behavior of the compression factor C as a function of α (i.e. the accelerating gradient). This is plotted in Fig.6, clearly displaying that there is actually an optimum value of α - about 0.25 - that maximizes the compression factor.

We repeated the simulations with the same injected beam and same slow wave structure as before, but changing now the gradient, i.e. applying 13 MV/m, corresponding to $\alpha = 0.44$, and increasing the structure length up to 6 m. The results are plotted in Fig.7: at an exit energy of 24 MeV the beam peak current is 1260 A with a longitudinal emittance of 80 keV·mm. As anticipated, at lower gradients the longitudinal emittance is better due to lower non-linear RF effects, hence the maximum peak current achievable is considerably higher.

The impact of these RF non-linear effects is clearly shown by the behavior of the longitudinal phase space distributions plotted in Fig.8 at various locations through the compressor.

The first diagram shows the energy phase distribution of the beam at injection into the compressor with a clear signature of the longitudinal space charge field action occurred from the photocathode surface up to the exit of the gun and further on through the drift to the compressor: some non-linearities are already present but mostly concentrated in the bunch tails, as expected. The second diagram is taken after the bunch has traveled a few wavelengths: since the injection is performed at 0° , most of the RF field action goes into producing an almost linearly correlated energy spread with particles in the tail being at higher energy than those in the bunch head. After some more RF periods – third diagram – the bunch starts being accelerated because of the phase slippage to higher phases – the beam is indeed slower than the wave at this point. At the same time the beam starts being bunched because of the phase space rotation caused by the linearly correlated energy spread. These two actions – bunching and acceleration – proceed actually together in a synergic way (see fourth and fifth diagrams) until an almost full rotation is achieved. The bunching couldn't be achieved at these moderate energies unless the average beam energy wouldn't be raised by acceleration to damp the outward pressure of the longitudinal space

charge forces, but unfortunately the acceleration process induces a phase space curvature that in turns increases the longitudinal emittance and prevents reaching much shorter bunch lengths. If the process is pushed up to its limit the beam reaches the exit of the compressor (sixth diagram, average energy 24 MeV) being over-compressed. This means that the energy spread is now no longer correlated and it could not be corrected by a further acceleration off-crest to higher energies – as is typically done in Linacs with magnetic compressors. We will show however in the next section an example of partial compression with further energy spread correction, that is possible by just adjusting the injection phase into the compressor.

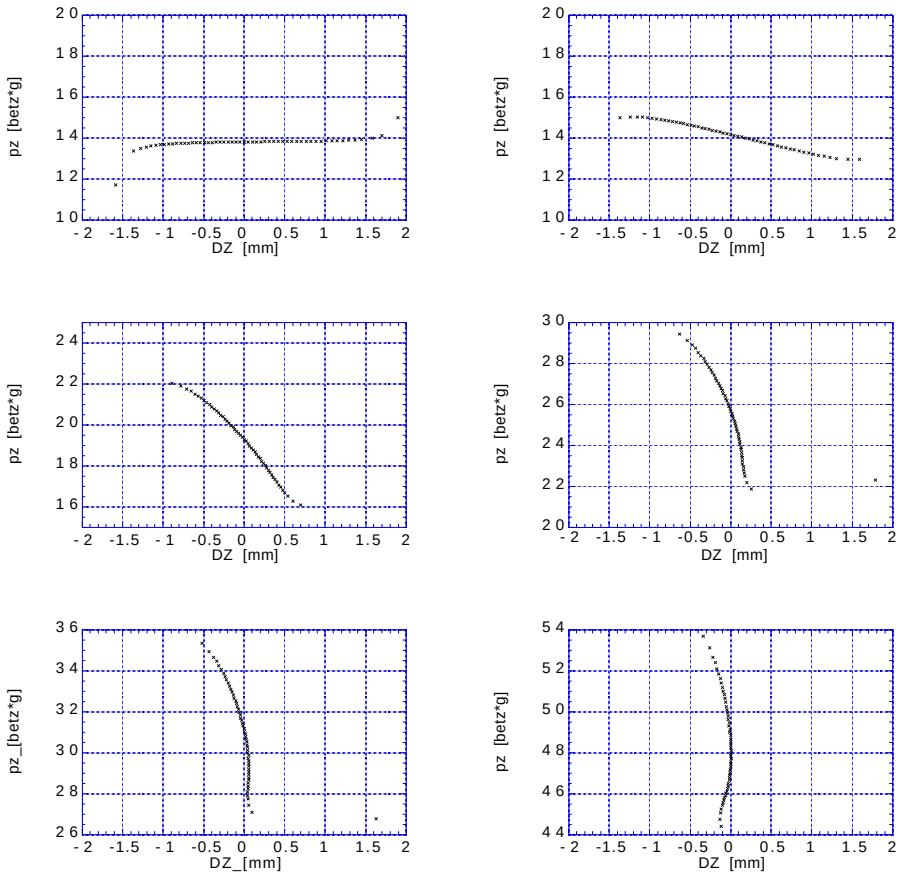

FIG. 8: Beam phase space distributions in the $(\Delta z, p_z)$ longitudinal plane at different locations through the 6 m long RF compressor (these are snapshots taken in time, as the code Homdyn is time-dependent). First diagram is for the beam at injection, last diagram is for the beam right at the compressor exit.

As discussed, the crucial feature of this method is the use of a slow RF structure such that the beam can be injected at a speed slower than that of the wave but it leaves the structure, after acceleration, being faster than the wave itself, i.e. at energies larger than the resonant gamma. The phase slippage is quite large during the compression, even up to 50-60° RF.

It would be possible to achieve such a phase slippage even in standard TW structures which are non-detuned, i.e. those having a wave phase velocity equal to the speed of light, for which the resonant gamma is actually infinity. In this structures the beam would be always

slower than the wave, so that it would not be possible not even to reach the resonant gamma by the end of the RF compressor.

We anyway checked the potentialities of RF compressors based on non-detuned structures just by running Homdyn on the LCLS injector scheme and using low injection phases in the first TW structure (i.e. we repeated the simulations presented in Fig.4-5 just by setting $\Delta k = 0$). The maximum peak current achievable is in this case 250 A at 28 MeV exit energy from the compressor, with a longitudinal emittance of 150 keV·mm.

3 RF RECTILINEAR COMPRESSORS WITH HIGHER HARMONIC CORRECTORS

Since the main limitation to the performances of the RF compressor basically comes from the RF nonlinearities, a possible solution to this is the use of higher harmonics superimposed to the main RF field, aimed at correcting locally the RF curvature and avoid the huge increase of longitudinal emittance which is, in turn, responsible of the limitation in the minimum bunch length achievable.

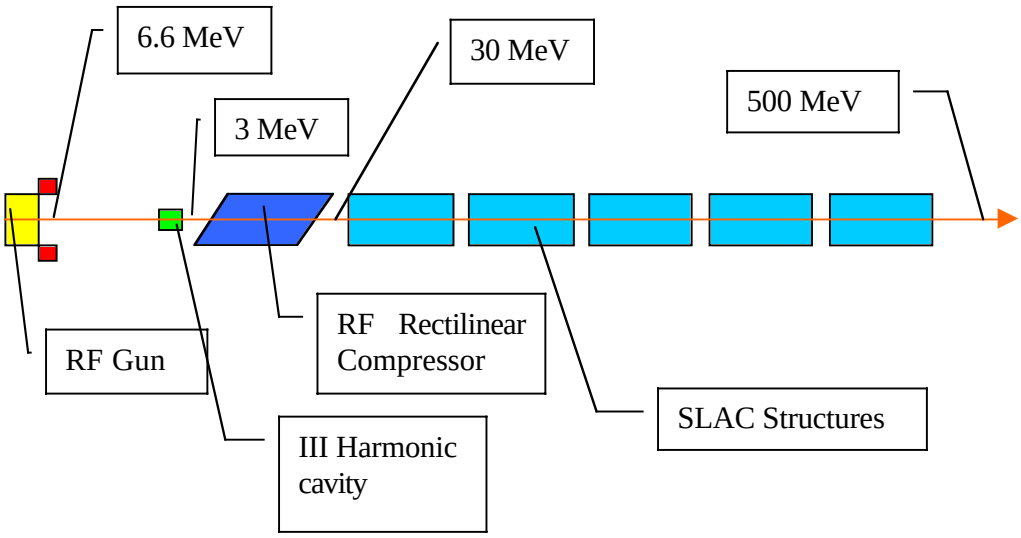

FIG. 9: Layout of a 500 MeV Linac based on a RF compressor with 3rd harmonic correction for the generation of a 2.3 kA beam with no use of magnetic compressors.

The superposition of higher harmonics is indeed not conceivable inside the same slow wave structure of the compressor: it couldn't even be placed after the compression if this is pushed up to the overcompression limit (as shown in Fig.8), hence it's natural to conceive a lay-out in which the higher harmonic structure is placed before the compressor, i.e. in the drift between the gun and the compressor itself. This drift (about 1 m long) is needed to accomplish the first part of the transverse emittance correction by properly focusing the beam plasma oscillations through it.

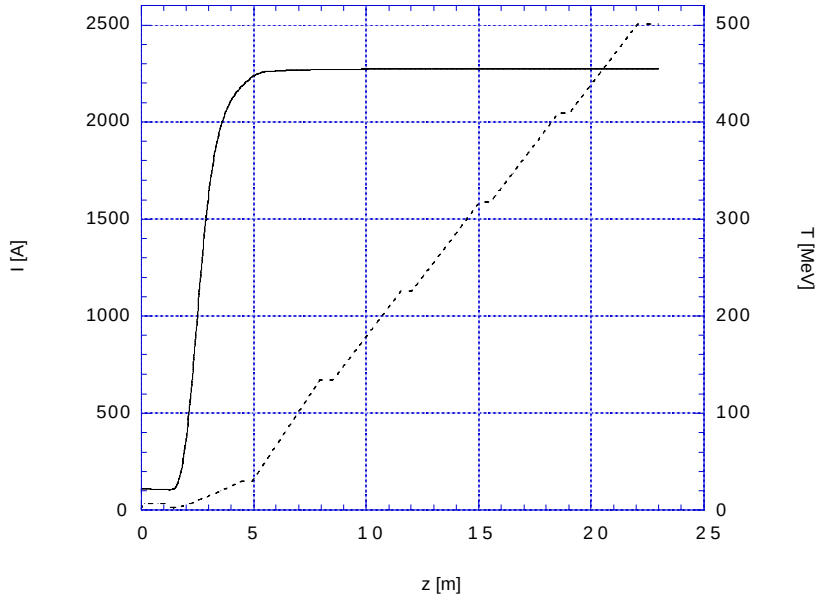

FIG. 10: Beam current (solid line, left scale, in A) and energy evolution (dashed line, right scale, in MeV) through a 500 MeV Linac with implementation of a RF rectilinear compressor and a 3rd harmonic corrector.

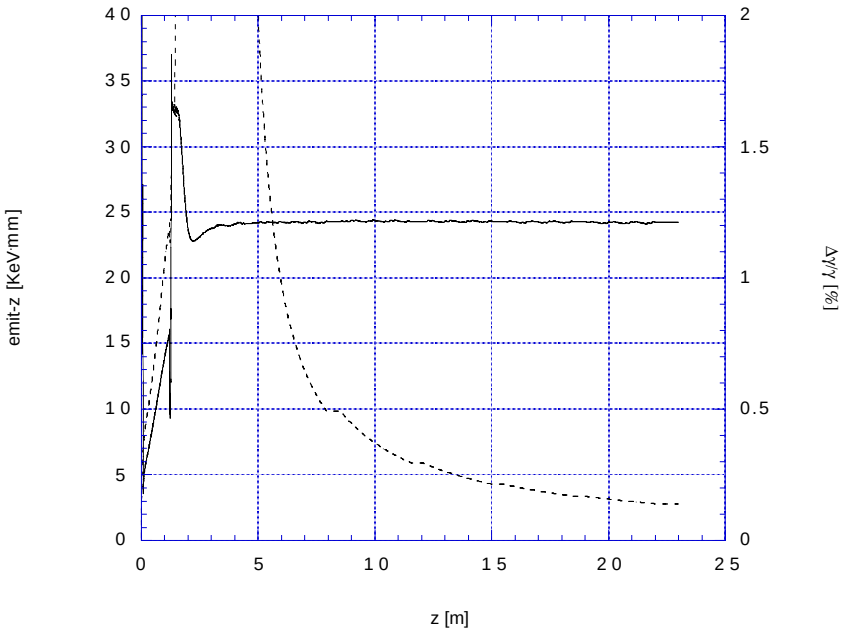

FIG. 11: Energy spread in % (dotted line, right scale) and longitudinal emittance in keV·mm (solid line, left scale) evolution as for Fig.10 .

We therefore consider here a lay-out as shown in Fig.9, with a short (7 cell) third harmonic structure placed right before the RF compressor, which is now followed by 5 standard 3 m long S-band SLAC TW structures in order to raise the beam energy up to 500 MeV, where the transverse space charge effects are expected to be negligible even for a 2 kA beam from the point of view of the emittance correction budget.

The RF compressor is set at same conditions as in the previous example, i.e. $\gamma_r = 27$ ($\Delta k = 0.07\%$), driven at 23 MV/m accelerating gradient, while the following structures are driven at 27 MV/m (but the first one, set at 31 MV/m).

The 3rd harmonic structure, being 8.2 cm long, is driven at 40 MV/m at a frequency of 8568 MHz (no detuning). Its role is indeed to pre-correct the RF induced curvature in the longitudinal phase space distribution as that shown in Fig.8: in order to achieve this task is actually enough that the total energy decrease induced by the 3rd harmonic structure is close to 1/9 of the total energy increase produced by acceleration into the RF compressor. This would in fact correct at least the second order derivative (scaling like n^2 , n being the harmonic number) of the phase space curvature, with a significant benefit to the longitudinal emittance.

This rule of the thumb would set a 3rd harmonic total energy decrease at 2.6 MeV, just one ninth of the total energy gain in the compressor, i.e. 23.5 MeV. From the simulations we found instead that the best results are obtained for an energy decrease of about 3.5 MeV, that corresponds to 40 MV/m acc. gradient. The reason for this disagreement is that the beam enters the compressor at 3 MeV, hence the energy gain and phase slippage are higher than before – as for the compression factor.

We should also notice that the exit energy from the compressor is in this case higher (30 MeV) than the case presented in previous section (see Fig.4): the reason is the higher phase slippage toward the RF field crest due to a lower injection energy in the compressor (3 MeV instead of 6.5 MeV).

Eventually the performances of the system are dramatically improved, thanks to the longitudinal emittance correction performed by the 3rd harmonic field, which brings it down to 25 keV·mm at the exit of the compressor, as opposed to 155 keV·mm without the 3rd harmonic correction. The beam current and energy throughout the Linac are plotted in Fig.10, while the energy spread and longitudinal emittance in Fig.11.

The final peak current value is 2.3 kA at full compression, with an energy spread of 0.13 % at the end of the Linac, and a normalized rms transverse emittance still at 0.6 mm·mrad. It's interesting noticing the longitudinal emittance correction mechanism developed by the 3rd harmonic structure, located at 1.2 m from the photo-cathode: it actually blows up the longitudinal emittance from 15 to 37 keV·mm, as plotted in Fig.11, because of the positive curvature induced to the longitudinal phase space distribution, which is however corrected further on by the negative curvature contribution produced by the main RF field in the compressor. This brings eventually back the longitudinal emittance to its final value of 24 keV·mm, which allows for a compression factor almost 3 times larger than that obtained in absence of the 3rd harmonic corrector (see Fig.4).

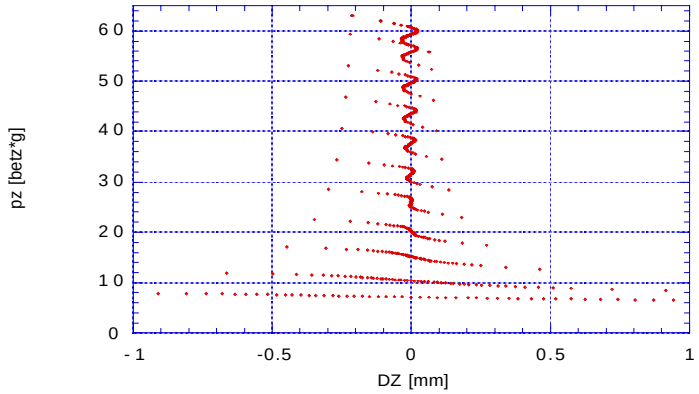

FIG. 12: Longitudinal phase space distributions taken at different times throughout the compressor for the case of total compression.

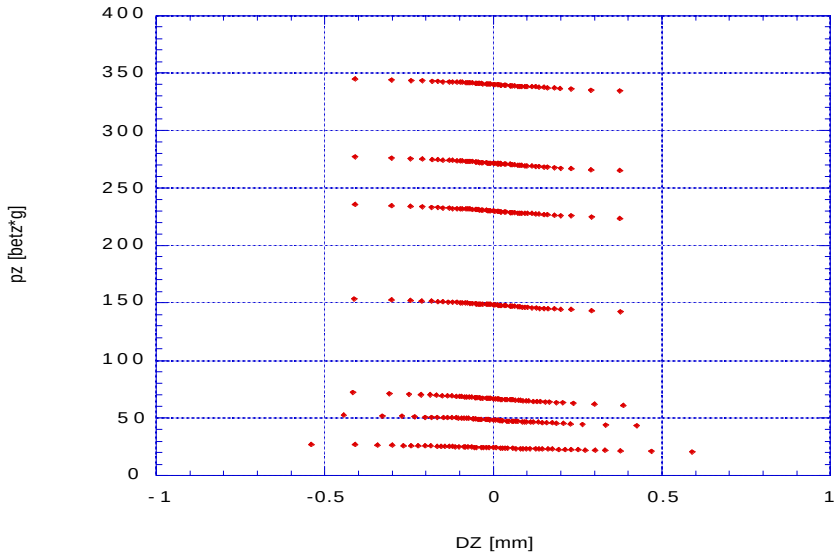

FIG. 13: Longitudinal phase space distributions taken at different times throughout the Linac for the case of partial compression.

The compression is pushed in this case up to its maximum limit, as shown in Fig.12, where the phase space distributions are plotted at various times throughout the compressor. The residual energy spread is totally uncorrelated to the phase, hence not recoverable any longer.

If the compression is performed partially so that a linear correlation is still present at the exit of the compressor between the energy and phase of particles in the bunch, this correlated energy spread can be corrected by running the beam slightly off-crest in the following accelerating sections: as an example, it is possible to produce a beam with peak current of 600 A and a final energy spread (at the Linac exit, 500 MeV) of 0.04 % . The evolution along the Linac of the corresponding phase space distributions is reported in Fig.13

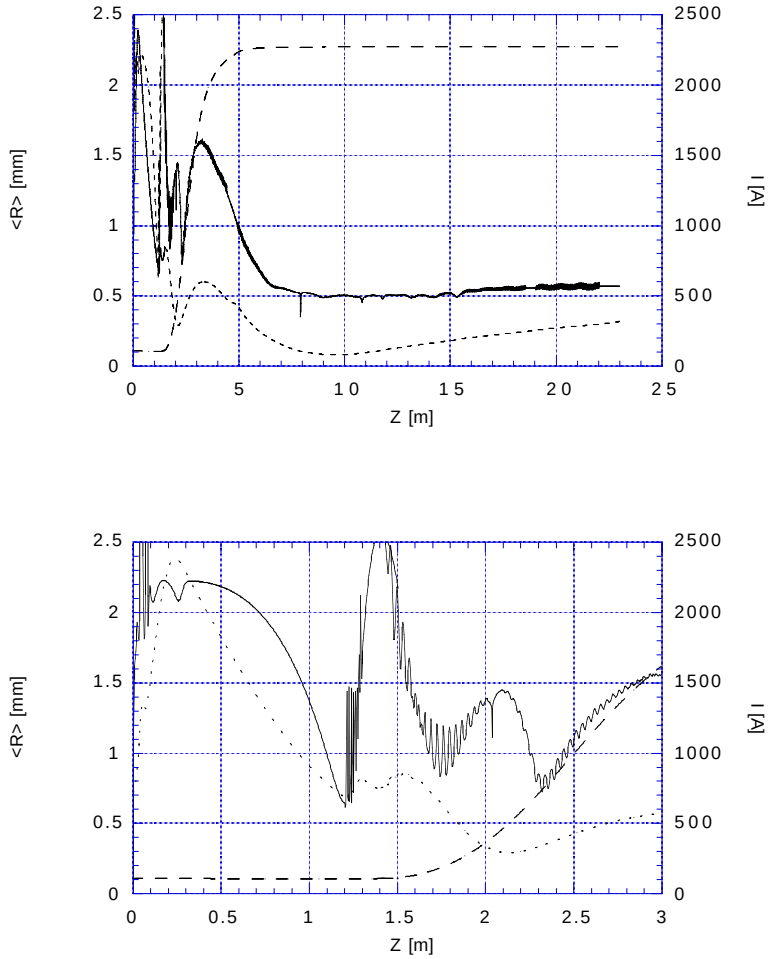

FIG. 14: Rms beam envelope in mm (dotted line, left scale) , rms normalized transverse emittance in mm·mrad (solid line, right scale) and beam peak current in A (solid line, right scale) along the Linac. The lower diagram shows the details of the upper one along the first 3 m of RF gun, drift, 3rd harmonic structure (from z=1.2 to z=1.28) and RF compressor (from z=1.4 to z=4.4)

The transverse dynamics is shown in Fig.14, where the rms beam envelope and normalized emittance are plotted along the Linac: the final emittance is still close to 0.55 mm·mrad, and this is again achieved by a careful setting of the field amplitudes and the locations of many solenoids placed around the RF compressor and the following two accelerating sections in order to keep focused the beam despite its increasing peak current. To this purpose, the RF compressor had to be placed closer to the RF gun exit, i.e. at 1.4 m far from the photocathode instead of 1.5 as for the LCLS nominal layout. Details of the transverse dynamics in this region are plotted in the lower diagram of Fig.14. No real systematic analysis has been done to optimize the transverse emittance up to 500 MeV: adding more solenoids in the last two accelerating sections would definitely help in taking the beam envelope better under control and getting a better emittance at the Linac exit.

4 RF RECTILINEAR COMPRESSORS WITH STANDING WAVE STRUCTURES

The analysis performed so far has been focused on the use of traveling wave structures, where the analytical treatment reported in the introduction strictly applies.

There is however a relevant interest also in applying this concept in the domain of Linacs based on standing wave structures. For this case an analytical theory of the rectilinear compressor has not yet been investigated in details. Nevertheless we expect to apply the previous treatment provided that only the forward travelling wave component of the standing wave is considered.

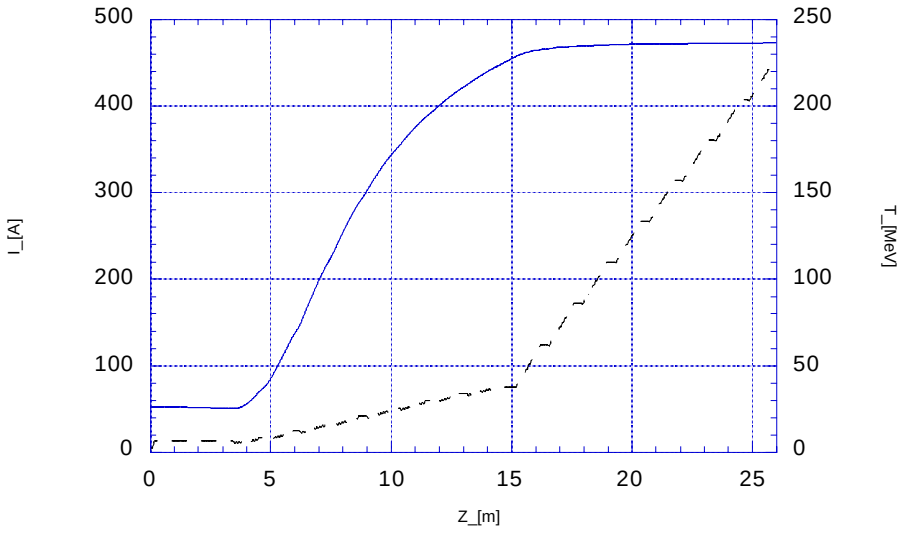

FIG. 15: Beam current (solid line, left scale) and energy evolution (dashed line, right scale) through the TESLA-FEL injector with implementation of a 11 m long RF compressor (first cryomodule).

We have applied for demonstration the rectilinear compressor concept to an injector beam line based on superconducting standing wave structures, as the one designed for the TESLA FEL project [9]. We have considered in this case a 1.3 GHz rf gun, 1.5 cells long, followed by two cryomodules each one containing 8, 1.3 GHz, 9 cells standing wave structures. A 1nC bunch is extracted from the cathode by a 20 ps long laser pulse in a 60 MV/m rf peak field and accelerated up to 6.6 MeV (γ_0=14) at the gun exit, resulting in a 50 A peak current (with 0.7 % energy spread and 0.6 mm-mrad rms transverse normalized emittance minimum). By detuning the first group of 8 cavities so to increase the wave number by 0.08 % , corresponding to a resonant gamma γ_r=25.5, and operating the detuned structures at 50 MV/m peak field, corresponding to α=1.8 for the forward travelling wave component, the expected compression factor results to be C=4.

The effectiveness of the rectilinear compressor scheme based on standing wave structures is clearly visible in Fig. 15 where the energy gain and the peak current are reported up to the end

of the second cryomodule. A compression ratio higher than 9 has been obtained without any attempt to optimize the longitudinal and transverse emittances nor the energy spread of the beam.

We can definitely speculate, nevertheless, that even in SW Linacs it should be possible to attain peak currents in excess of 1 kA by implementation of higher harmonic correctors as it was shown in previous section.

5 CONCLUSIONS

On the basis of the very preliminary analysis presented in this paper we may conclude that the use of RF rectilinear compressor can be very helpful in the design of SASE X-ray FEL drivers, either in alternative to magnetic compressors, or to alleviate the criticality of these devices, i.e. in order to avoid multi-staged magnetic compressors that appear critical in those projects.

In fact, we have shown here that peak currents in excess of 2 kA are achievable with the use of properly designed RF compressors. Since there is no systematic study performed so far on these devices we might speculate that one should be able to reach even higher current levels (> 3 kA ?). In case one is aiming at higher currents the use of a magnetic compressor could be unavoidable, but its criticality should be diminished by the lower compression factor required to it – because the beam would already have more than 1 kA of peak current at its entrance.

In order to summarize all the different examples presented in this paper, we listed in Table 1 the different options available: this enlighten the flexibility of this method that can be applied in several different situations, from Linacs based on TW room temperature structures to Superconducting SW Linacs, at almost any frequency of interest in these designs (included plasma accelerators, where the method was firstly conceived).

TABLE 1. Performances of RF Rectilinear Compressors.

Type of structure	Peak Current [A]	Energy spread [%] @ 500 MeV	Long.emittance [KeV·mm]
zero detuning @ S-band TW	250	0.1	150
0.07% detuning @ S-band TW	870	0.3	155
plus 3rd Harmonic	2300	0.13	25
plus 3rd Harmonic partial compression	600	0.04	25
0.08% detuning @ L-band SW	470	not optimized	not optimized

6 ACKNOWLEDGMENTS

We acknowledge very helpful discussions with G.D'Auria and C.Rossi on slow-wave structures for the RF compressor.

7 REFERENCES

[1] M. Ferrario, T. C. Katsouleas, L. Serafini, I. Ben-Zvi.,"Adiabatic Plasma Buncher", in publication on *IEEE Trans. on Plasma Science*, **28**, no.4 (2000).

[2] C. Clayton and L. Serafini, *IEEE Trans. on Plasma Science* **24**, p.400 (1996).

[3] C.S. Liu, V. K. Tripathi, *Interaction of Electromagnetic Waves with Electron Beams and Plasmas ,* World Scientific Publ., 1994, pp. 60-63.

[4] J. Arthur et al., *Linac Coherent Light Source (LCLS) Desing Study Report*, SLAC-R-251, Apr. 1998.

[5] M. Ferrario, J. Clendenin, D. Palmer, J. Rosenzweig, L.Serafini,, "HOMDYN study for the LCLS photoinjector", in publication on *Proc. ICFA Workshop on The Physics of High Brightness Beams*, Ed. J. Rosenzweig and L. Serafini, World Scientific Publ., (2000).

[6] M. Ferrario, A. Mosnier, L. Serafini, F. Tazzioli, J.M. Tessier, *Particle Accelerators* **52**, p.1 , (1996).

[7] L. Serafini and J. B. Rosenzweig, *Physical Review* **E 55**, p.7565 (1997).

[8] D. H. Dowell, T. D. Hayward, A. M. Vetter, *IEEE Cat.* no. 95CH35843, p.992 (1996)

[9] Conceptual Design of a 500 GeV e+e- Linear Collider with Integrated X-ray Laser Facility, Ed. R. Brinkmann, G. Materlik, J. Rossbach, A. Wagner, DESY-1997-048

[10] The analytical model takes indeed into account only initial energy and phase spreads which are uncorrelated and uniformly distributed around the average injection energy and phase. The simulations are instead done with injection conditions for the beam (see fig.8) that imply correlated longitudinal distributions with only partial fill-up of the longitudinal phase space: this may be the reason why the analytical model tend to underestimate the compression factor.